NANO LETTERS

2007
Vol. 7, No. 2
247−253

A Parallel Approach for Subwavelength Molecular Surgery Using Gene-Specific Positioned Metal Nanoparticles as Laser Light Antennas

Andrea Csaki,[†] Frank Garwe,[‡,||] Andrea Steinbrück,[†] Gunter Maubach,[†,⊥] Grit Festag,[†] Anja Weise,[§] Iris Riemann,[‡,⊗] Karsten Kȍnig,*[,‡,⊗] and Wolfgang Fritzsche*[,†]

Institute for Physical High Technology, P.O. Box 100239, 07702 Jena, Germany, JenLab GmbH, Schillerstrasse 1, 07745 Jena, Germany, and Friedrich-Schiller-University, Institute for Human Genetics and Anthropology, 07745 Jena, Germany

Received August 22, 2006; Revised Manuscript Received December 20, 2006

ABSTRACT

An optical technique for the parallel manipulation of nanoscale structures with molecular resolution is presented. Bioconjugated metal nanoparticles are thereby positioned at the location of interest, such as, e.g., certain DNA sequences along metaphase chromosomes, prior to pulsed laser light irradiation of the whole sample. The nanoparticles are designed to absorb the introduced energy highly efficiently, in that way acting as nanoantenna. As result of the interaction, structural changes of the sample with subwavelength dimensions and nanoscale precision are observed at the location of the particles. The process leading to the nanolocalized destruction is caused by particle ablation as well as thermal damage of the surrounding material.

Nanotechnology implies the control of nanomaterials and nanodevices. Thereby, this field depends on the availability of methods for manipulation at the nanoscale. Chemical approaches based on specific molecular binding and self-organization provide a tremendous potential in the preparation of a variety of possible structures reaching high levels of complexity. Thereby, a controlled manipulation of individual molecular species, usually in a mixture of quite similar molecules, is an often required but difficult task. Especially, the selection of the molecule of interest and further on the localization of the region to be manipulated (e.g., by cutting or destroying) represent a limiting factor.

One approach uses microscopic techniques. A highly focused laser beam is an established tool for manipulation at the microscale,[1] achieving cut widths of subwavelength dimensions.[2] Another truly nanoscopic tool is the AFM, which can be used for manipulations at the molecular scale.[3] Although these microscopic methods provide an impressive control over the location of manipulation, they are limited regarding their degree of parallelization: they manipulate one molecule at a time with a throughput of probably tens per day and require qualified personnel and sophisticated equipment.

For applications toward the manipulation of all structures (such as molecules) with a given property in a sample, the above-mentioned microscopic methods are insufficient. This task requires a parallel approach such as nature demonstrates in the case of DNA restriction enzymes that manipulate (cut) all DNA molecules with a specific sequence. Although the creation of similar artificial autonomous and active nanomanipulators seems infeasible today, there are approaches that combine the basic feature of manipulation at the nanoscale with an external control: an established example represents the photothermal therapy, where active reagents (photoactive compound) are positioned at a certain localization prior to activation by an external trigger (i.e., light). As result, these cells or tissues are damaged due to produced toxic products. The same basic principle of internal nanoscale converter and external trigger is utilized in several approaches to thermal therapy of cancer, where nanoparticles represent the active elements transforming, e.g., magnetic fields[4] or laser light,[5]

* Corresponding authors. E-mail: fritzsche@ipht-jena.de (W.F.), karsten.koenig@ibmt.fraunhofer.de (K.K.).
† Institute for Physical High Technology.
‡ JenLab GmbH.
§ Friedrich-Schiller-University.
|| Present address: Institute for Applied Physics (IAP), Ultra-optics Group, Albert-Einstein-Strasse 15, 07745 Jena, Germany.
⊥ Present address: IBN Singapore, 31 Biopolis Way, The Nanos #04-01 Singapore 128669.
⊗ Present address: Fraunhofer Institute of Biomedical Technology (IBMT), Ensheimer Strasse 48, 66386 St. Ingbert, Germany.

10.1021/nl061966x CCC: $37.00
Published on Web 01/24/2007

Scheme 1. Overview over Highly Localized Chromosome Manipulation Using Site-Directed Positioning of Particle-Based Nanoantennas.

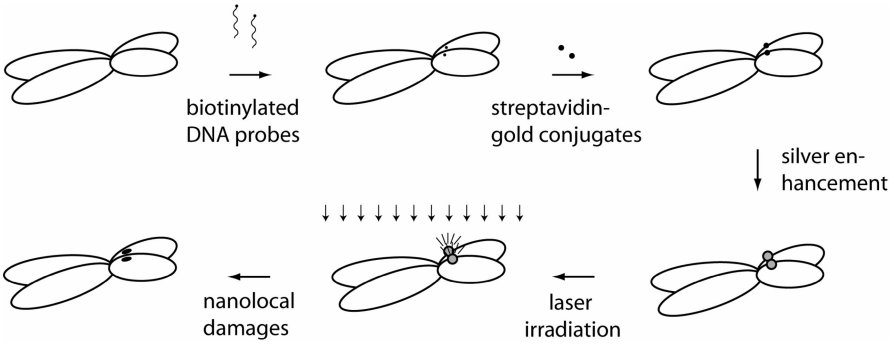

Biotinylated DNA probes are utilized for gene-specific labeling. The position of the labels depends on the addressed target region; in this paper, centromeric (central) and telomeric (terminal) sequences have been used. These biotinylated sites are targeted by streptavidin−gold conjugates. The immobilized gold particles are then silver-enhanced (in order to tune their absorbance band, cf. Figure 1). Laser irradiation of the whole preparation leads to energy absorption only at the particles, resulting in nanolocalized damages only at the targeted sites.

into tissue-damaging heat. In the case of photonic applications, longer wavelengths (NIR) are preferred due to the much better penetration behavior (because of less absorption by typical biological material).[6,7] This technique can also be brought to the cellular or even molecular level, as demonstrated in the case of proteins adsorbed onto nanoparticle surfaces[8] or particles bound to protein aggregates.[9]

There are many examples for the defined conjugation of nanoparticles on the single molecule level.[10,11] The particles were thereby often used as a label for topographic (AFM) or optical contrast and also utilized for DNA chip detection.[12] Besides this application as a rather passive label, the conversion of external energy into heat is another interesting way to use these particle conjugates. Such a remote heating was demonstrated in the case of DNA and the use of inductive coupling of a radio frequency magnetic field, achieving a warming that leads to dissociation of double-stranded DNA.[13] In this Letter, we go beyond the described DNA treatment in two ways, thereby opening novel and innovative possibilities for molecular manipulations. We show that external heating of nanoparticles can even be utilized to induce DNA damage (in a highly localized fashion) that could be useful for local manipulation and that light instead of a magnetic field can be used for destructive action at the nanoscale following the references discussed before.[5,8] The application of light allows for a higher degree of control because not only certain molecules (which are labeled) but also only certain substrate regions (which are irradiated) are addressed. We chose metaphase chromosomes as an example of a biologically relevant state of DNA packed by proteins and applied sequence-specific binding of nanoparticles using in situ hybridization techniques[14] (Scheme 1). To be compatible with medical application in, e.g., tissue, wavelengths in the near-infrared are preferred. Therefore, the surface plasmon resonance band of the used gold nanoparticles was tuned by a silver shell deposition to the required value in the 400 nm range for two-photon excitation using a near-infrared laser. A nanoscale localization of the damaging effect was realized by using short (fs) laser pulses because the degree of localization depends on the ratio of exposure duration to thermal relaxation time of the target structure.[15]

The specific interaction of laser light with metal nanoparticles due to their surface plasmon resonance leads to local temperature increase and can eventually result in structural changes and irreversible destruction of the particles.[16−18] To utilize this process for biomolecular manipulation, the laser parameters had to be adapted to the metal nanoparticles and the biological environment used. For biological environments, wavelengths approaching the IR part are preferred due to lower absorption. On the other hand, the resonance frequencies of gold and silver nanoparticles are around 520 and 400 nm, respectively. To fulfill both requirements, a two-photon excitation at 400 nm with laser irradiation at 800 nm was utilized. Because gold nanoparticle labeling is widely established in biological microscopy for decades, we decided to use specific binding of gold particles prior to shifting the resonance wavelength of the gold particles at originally around 520 nm toward 400 nm by deposition of a silver shell. This optical effect of an additional metal shell on nanoparticles is known[19] and was adapted using optical (Figure 1a) and ultramicroscopic (Figure 1b,c) characterization. The process (scheme in Figure 1a, top) is based on the catalytic activity of gold and subsequently silver surfaces toward a reduction of silver ions from solution that is confined to the growing particles.[20] AFM studies demonstrate thereby the high specificity of silver deposition only at the gold nanoparticles with no detectable unspecific background signal (Figure 1b,c). Such particles exhibit a resonance band at a wavelength between the pure silver and gold particles, and the exact position depends mainly on the thickness of the silver shell (Figure 1a).[21]

After adapting the particle resonance to the used laser, first, tests in a biological environment were conducted. Therefore, gold nanoparticles had to be attached to DNA. To allow for a homogeneous coverage of the used DNA samples, a DNA-specific attachment was applied. It is based on electrostatic interactions between the negatively charged DNA and

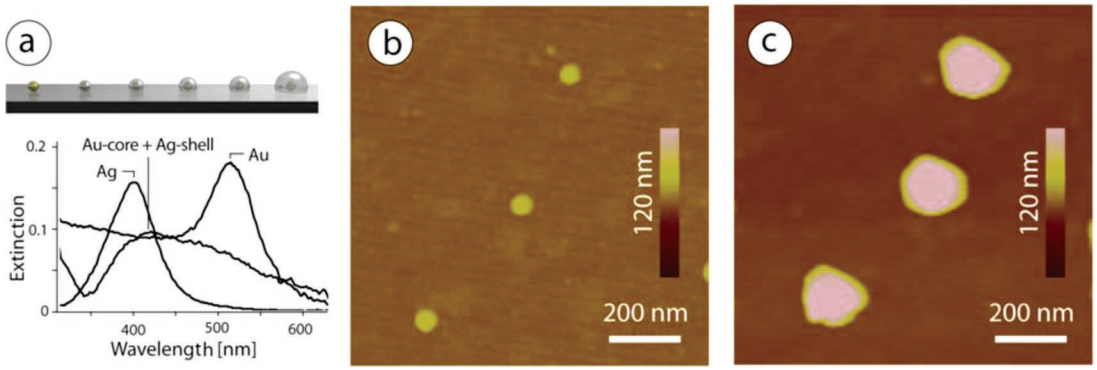

Figure 1. Tuning the surface plasmon resonance wavelength by chemical modification of particles: gold nanoparticles with an absorption band at about 520 nm were covered by a silver shell, thereby shifting the absorption wavelength toward 400 nm. (a) Scheme (top) and spectra of pure gold or silver particles as well as gold−silver core−shell structures illustrating the changes in the spectrum. (b) AFM images of immobilized gold nanoparticles before and (c) after silver shell growth.

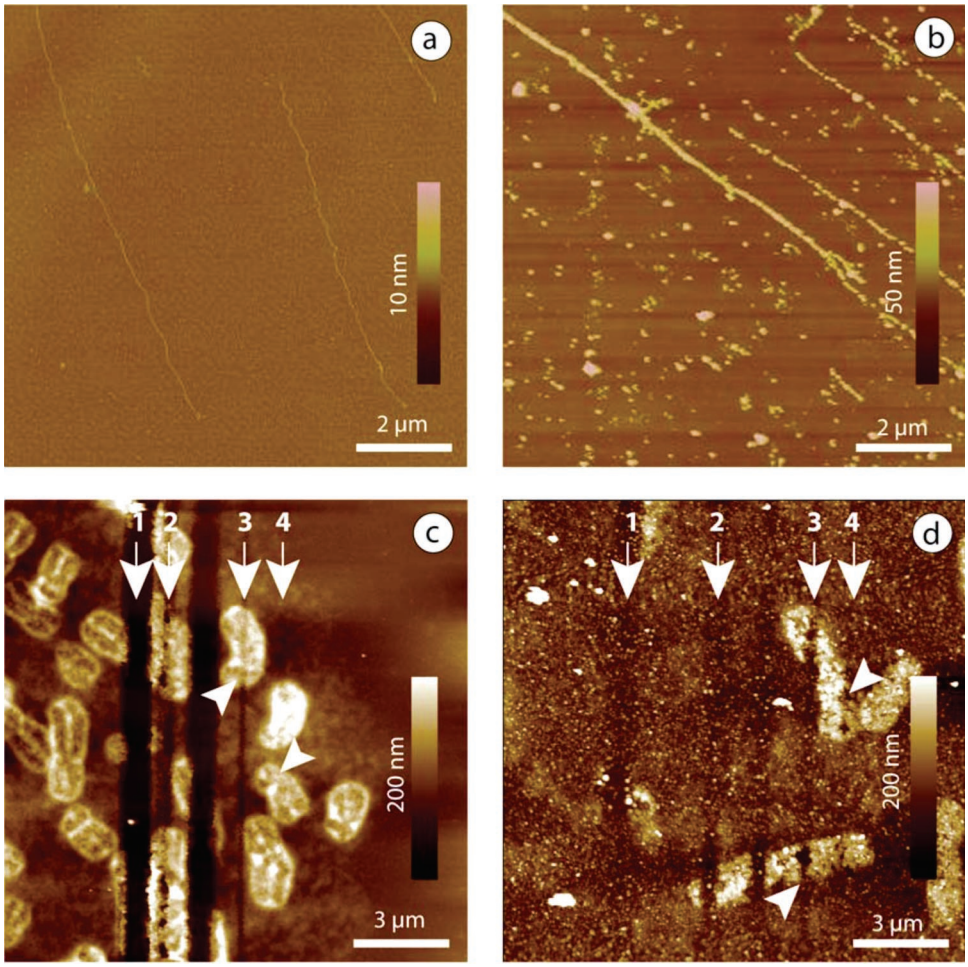

Figure 2. Combining metal nanoparticles and biological targets. Positively charged gold nanoparticles (20 nm diameter) adsorb electrostatically onto DNA, as demonstrated by AFM imaging of immobilized Lambda DNA before (a) and after (b) nanoparticle treatment (note the different height scales). This process was used to bind such particles to metaphase chromosomes prior to silver enhancement as introduced in Figure 1, leading to gold−silver core−shell particles of about 60 nm final diameter. The application of different levels of laser power in a line-scan mode (1−77, 2−27, 3−11, 4−7 mJ/cm^2) onto chromosomes without (c) and with (d) metal particles was studied. It demonstrated a higher efficiency for particle-decorated chromosomes, as, e.g., visible in the effects of line 4 clearly visible in (d) but not in (c).

positively charged gold nanoparticles of 20 nm diameter (Genogold, BBI). AFM studies of immobilized *Bacteriophage lambda* DNA were conducted in order to study this process (Figure 2a,b). The images demonstrate a highly specific attachment of the particles along the DNA (as evident in the enhanced height of the rod-like structures in Figure 2b compared to the naked DNA before in Figure 2a). Besides DNA that is apparently nearly continuously covered by the

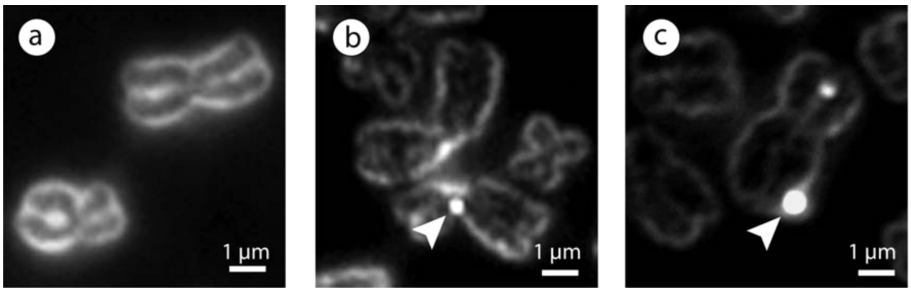

Figure 3. Optical dark-field imaging for the monitoring of particle binding (marked by arrow heads) onto immobilized metaphase chromosomes. (a) Chromosomes before binding. (b) DNA-probe targeting the centromeric region (centromere) was applied. (c) DNA sequence located in the terminal (telomere) region of chromosomes was particle-labeled and silver-enhanced up to a diameter of about 100 nm.

particles, also strands with a more discontinuous coverage are visible (comparable to the results on DNA immobilized on silicon oxide substrate described elsewhere[22]).

This particle-labeling technique was now applied to chromosomes, representing a packing state of DNA in eukaryotic cells. To test the effect of light onto these structures and study possible enhancement effects of metal nanoparticles, standard human metaphase chromosome spreads with or without particle labeling were laser irradiated. The gold nanoparticles used for labeling were subjected to a silver enhancement step (as described before) to adjust the particle plasmon resonance wavelength to about 400 nm to apply a two-photon excitation using an 800 nm fs laser (for details, see Supporting Information). The irradiation experiment addressed two points: to identify conditions that allow for (a) coupling sufficient energy into the particles in order to induce damages there and (b) to minimize damages at other regions due to absorption of the biological matrix (such as proteins or cell debris). A line-scan mode was chosen to compare various energy levels and to provide also internal controls by the adjacent regions that were not irradiated. AFM imaging reveals the microtopography of the samples after laser treatment (Figure 2c,d). Both samples show stripe-like zones of damage pointing to laser effects. To study the influence of the introduced power, four different laser fluencies were applied between 77 and 7 mJ/cm^2 (complemented by an additional central strip for adjustment purposes). Without particles, 77 mJ/cm^2 led to extended damage both on the background and at the chromosome structures, whereas 27 mJ/cm^2 are less significant, 11 mJ/cm^2 hardly detectable, and the last line at 7 mJ/cm^2 shows no effect (Figure 2c). For the particle-labeled chromosomes, all lines are visible at the chromosomes (although less clear due to the surface roughness induced by the nanoparticle adsorption). However, the line with 11 mJ/cm^2 is not detectable at the background, pointing to a process window regarding the laser power that minimizes unspecific damages of the matrix but allows for effects at the chromosomes.

After demonstrating the interaction between laser light and nanoparticles even in a biological environment, we addressed the controlled positioning of the particles. DNA-modified particles are known to be able to bind complementary DNA sequences that are either in solution[23,24] or immobilized.[25,26] We applied a standard two-step procedure using biotinylated DNA for in situ hybridization prior to a subsequent incubation with streptavidin−gold conjugates in order to minimize any influence of the particle onto hybridization efficiency. The first step was labeling the metaphase chromosome with a DNA probe complementary to the defined target DNA sequence. Target DNA positioned in the primary chromosome constriction (centromere)[27] or at the terminal chromosome ends (telomere)[28−33] were utilized and subsequently conjugated to streptavidin−gold. The positioned gold nanoparticles were then silver enhanced in order to tune their optical absorption to 400 nm. This step increased their size to about 60 nm and made them clearly visible in optical dark-field contrast for characterization of the hybridization efficiency. Figure 3 shows typical metaphase chromosomes before (a) and after (b,c) particle labeling and silver enhancement, with the particle labels appearing as bright spots. The chosen sequences positioned the particles at either the centromere (b) or the telomere (c) region of the chromosomes.

The next and final step was to combine the preliminary experiments and to irradiate sequence-specific particle-labeled chromosomes in order to demonstrate the proposed approach for nanoscale manipulation of a biological sample. Therefore, chromosomes were labeled with gold nanoparticles prior to silver enhancement, as shown in Figure 4. To characterize the effect of laser irradiation, the samples were imaged by AFM before (Figure 4a). The silver-enhanced nanoparticles appear as protrusions (bright in the height contrast), which are usually above the background roughness of the chromosome surface. By using optical dark-field contrast (complementary information), it was possible to assign surface features to either metallic or other (biological) structures. AFM allows also high-resolution imaging of regions around nanoparticle labels (Figure 4b). The characterized chromosomes were irradiated and thereafter again imaged by AFM (Figure 4c). Although the overall structure of the chromosome was well preserved (no significant unspecific absorption), the known locations of particle labels showed dramatic changes at closer inspection (e.g., Figure 4d): the protrusions were transformed into nanoscale cavities, pointing to highly localized effects. Measurements utilizing high-resolution imaging (Figure 5a) confirm that the cavities are of subwavelength dimensions.

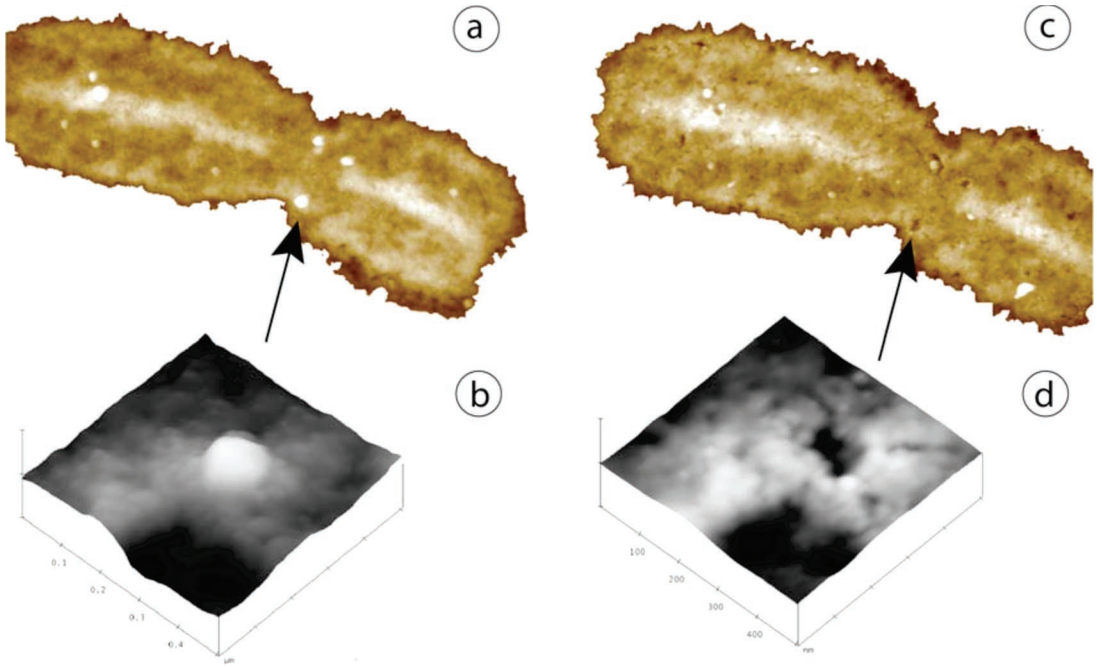

Figure 4. Highly localized energy conversion at sequence-specific bound nanoparticles on metaphase chromosomes. AFM images: overviews (a,c) and 500 nm × 500 nm zooms (b,d) of the marked regions. Particles targeting certain DNA sequences on a chromosome before (a,b) and after (c,d) laser irradiation. The irradiation results in a disappearance of the particles in the AFM image and the formation of nanocavities at these locations (cf. d).

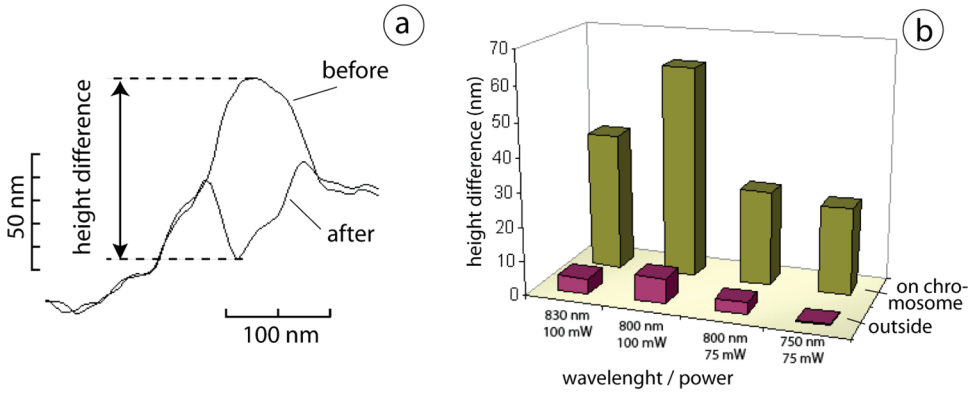

Figure 5. Influence of laser parameters onto the labeled target regions. (a) Cross sections of the particle-labeled chromosome region shown in Figure 4b,d, revealing the effect of laser irradiating leading to a height difference. (b) This height difference was measured for ensembles of particles situated both on chromosomes (back row) and on the substrate around the chromosomes (front row) for various combinations of the laser parameters wavelength and power (overall particle number: 64).

These results demonstrate the feasibility of the approach utilizing metal nanoparticles as sequence dependently positioned antennas in order to induce nanoscale damages in genetic material. What are the limits? The success depends on the efficiency of nanoparticle labeling, which is mainly determined by the efficiency of DNA hybridization as in all in situ hybridization approaches. The background signal is determined by the unspecific binding of the target DNA as well as the gold nanoparticle labels: it is crucial in cases of particles positioned along the chromosomes but on wrong positions, but less important when adsorbed to the substrate in between the chromosomes (as visible in the dark-field image in Supporting Information). As known from decades of experiences in biology, optimization of procedures for passivation ("blocking") the sample surface against unspecific binding could further improve the specificity of the binding process.

What happens during the destructive process? Does the heat induced in the particles lead to complete particle ablation (cf. Scheme 2b), or is the particle simply embedded into the chromosome matrix due to sinking in a melted matrix (Scheme 2c)? Measuring the changes in topography (measured in height) induced by the laser treatment onto nanoparticle-labeled locations could reveal some information: for the site shown in high resolution in Figure 4b,c, the cross-sections reveal a height difference of ca. 60 nm (Figure 5a). This value could be explained by complete ablation as well as purely sinking of the still intact particle, as well as any combination of both processes. Studies of particles processed on heat-sensitive polymeric substrates point to the possibility

Scheme 2. Possible Mechanisms for the Destructive Activity of Laser-Activated Metal Particles Acting as Nanoantenna.

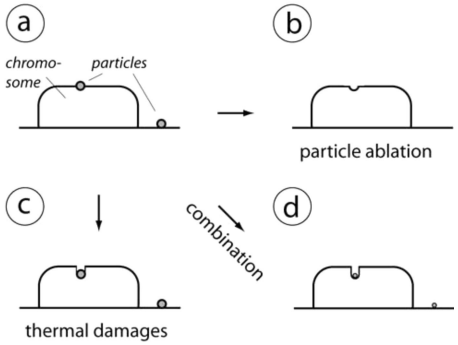

(a) Typical sample with particles sequence specifically bound to certain DNA regions on the chromosomes as well as particles unspecifically adsorbed to the substrate. (b) In the case of extensive particle ablation,[17,18] the particles on the substrate would disappear, and particles on the chromosome would lead to cavities. (c) On the other hand, heated particles could sink into the chromosome material. As a result, particles on the substrate would remain, but particles on the chromosome would disappear into the chromosome, leading to the formation of a cavity. (d) There is also the possibility for a combination of the processes of ablation (b) and heat-induced sinking (c), resulting in cavity formation on chromosomes as well as in height loss of particles adsorbed around the chromosomes.

of heat-induced melting of the substrate in the immediate vicinity of the label and subsequent sinking of the particle (Garwe et al., unpublished results). Another complementary experiment would be to study the laser effect on particles on substrates that cannot melt in order to reveal the behavior of the particle. Such experiments were included in the experiments with the chromosomes by metal nanoparticles unspecifically adsorbed to the substrate regions outside of the chromosomes (cf. dark-field image in Supporting Information). AFM images before and after laser irradiation allowed for the measurement of structural (i.e., height) changes both for particles located at chromosomes and outside of chromosomes. The results are presented in Figure 5b as the second set of experiments for a wavelength of 800 nm and a fluency of 28.7 mJ/cm^2. Clearly visible is the difference in structural changes at nanoparticles located on the chromosome (height change of about 60 nm) compared to particles situated around the chromosomes (height changes of less than 10 nm). These results point to a partial ablation of the particles (as detected outside of the chromosomes) in combination with a significant sinking of the remaining particle structure into the chromosome material. This observation leads us to the assumption that the processes depicted in Scheme 2d are a correct description: the nanoparticles are slightly ablated, but the main contribution to damages on the chromosomes is due to heat-related sinking of the particles into the chromosome material.

How can this effect be controlled? The influence of the laser power was studied using again measurements on the laser effect on particles. Utilizing the same (800 nm) wavelength but reducing the fluency from 28.7 to 21.8 mJ/cm^2 results in a decrease of the laser effect by ca. 50% (Figure 5b): for this reduced power, particles on the chromosome show a height difference of 31.5 $\pm$ 18.7 nm (compared to 61.7 $\pm$ 10.5 nm for 28.7 mJ/cm^2 fluency, 95% confidence), and particles immobilized directly on the glass substrate exhibit a height loss of 3.4 $\pm$ 2.0 nm (compared to 7.5 $\pm$ 12.7 nm for 28.7 mJ/cm^2 fluency, 95% confidence). These results demonstrate the influence of the laser power onto the achieved localized surface modifications and point to a simple approach to control the extent of the induced damages.

Another set of experiments was aimed at the question of the wavelength-dependence of the observed effects: is it possible to selectively address only metal nanostructures that show an absorption peak at the laser wavelength? If this principle would work, an extension of the approach using different laser wavelengths enables multiplexing using particles with different absorption properties, e.g., utilized for labeling different DNA sequences (A, B) with differently absorbing particles, leading, e.g., to the choice of selectively knock-off gene A with a red laser and/or gene B with a green laser. To investigate the wavelength dependency, particle-labeled chromosomes were irradiated using the same power but different wavelengths. As shown in Figure 5b, a shift in wavelength of 30 or 50 nm had a significant influence on the efficiency of energy conversion (and therefore the damaging effect) compared to the effect of laser light of the absorption band of 800 nm. A shift by 30−830 nm decreases the damage by one-third, shifting 50 nm to lower wavelengths (750 nm) even leads to a nearly two-third decrease. The observed decreases apply roughly to the same extent to particles at the chromosomes as well as to those immobilized directly on the substrate surface.

How precise is the presented DNA manipulation technique? Damaging zones of several tens of nanometers are observed on the chromosomes (Figures 4, 5). The dimensions are probably influenced by the final particle size of ca. 60 nm. Using smaller particles (such as Au−Ag core−shell or even Ag) in the lower nanometer range could significantly minimize the size. Another parameter influencing the extent of damages would be the laser power, as demonstrated in the experiments presented in Figure 5b.

The spatial arrangement of DNA in the vicinity of the particles is a key parameter. The high DNA packing in chromosomes results in more DNA situated nearby the particle compared to the case of isolated and extended DNA molecules; the utilization of more extended states of chromatin would be the way to achieve higher resolution. On the other hand, because of the high packing, some targeted sites were probably not accessible for the particle labeling and could therefore not be addressed. Again, smaller labels are the answer because they are known for better penetration abilities.

Summarizing, we present here a novel approach to utilize metal nanoantennas in order to manipulate DNA sequence specifically by optical means with a subwavelength resolution. The procedure is highly parallel and can be potentially multiplexed by addressing several different sequences (such as genes). Applications are envisioned in DNA analytics

(such as DNA fingerprinting or mutation analysis) as well as single-molecule manipulations.

Acknowledgment. This work was supported by the BMBF in the framework of the Nanobiotechnology initiative (NanoCut FKZ 0312013). We thank Michael Köhler for his help with initiation of the project and valuable discussions, Arne Bochmann and Gereon Hüttmann for assistance with laser experiments, and Uwe Klenz for help with graphics rendering.

Supporting Information Available: Materials and Methods. Optical dark-field micrograph of labeled metaphase chromosomes. This material is available free of charge via the Internet at http://pubs.acs.org.

References

(1) Greulich, K. O. *Micromanipulation by Light in Biology and Biomedicine: Laser Microbeam and Optical Tweezers*. Birkhäuser: Basel, Switzerland, 1998.
(2) König, K.; Riemann, I.; Fritzsche, W. *Opt. Lett.* **2001**, *26*, 819−821.
(3) Lieber, C. M.; Kim, Y. *Adv. Mater.* **2004**, *5*, 392−394.
(4) Hilger, I.; Kiessling, A.; Romanus, E.; Hiergeist, R.; Hergt, R.; Andrä, W.; Roskos, M.; Linss, W.; Weber, P.; Weitschies, W.; Kaiser, W. A. *Nanotechnology* **2004**, *15*, 1027−1032.
(5) Hirsch, L. R.; Stafford, R. J.; Bankson, J. A.; Sershen, S. R.; Rivera, B.; Price, R. E.; Hazle, J. D.; Halas, N. J. *Proc. Natl. Acad. Sci. U.S.A.* **2003**, *100*, 13549−13554.
(6) Denk, W. M.; Stickler, J. H.; Webb, W. W. *Science* **1990**, *248*, 73−76.
(7) König, K. Cellular Response to Laser Radiation in Fluorescence Microscopes. In *Methods in Cellular Imaging*; Periasamy, A., Ed.; Oxford University Press: New York, 2001.
(8) Hüttmann, G.; Radt, B.; Serbin, J.; Lange, B. I.; Birngruber, R. *Med. Laser Appl.* **2002**, *17*, 9−14.
(9) Kogan, M. J.; Bastus, N. G.; Amigo, R.; Grillo-Bosch, D.; Araya, E.; Turiel, A.; Labarta, A.; Giralt, E.; Puntes, V. F. *Nano Lett.* **2006**, *6*, 110−115.
(10) Csáki, A.; Maubach, G.; Born, D.; Reichert, J.; Fritzsche, W. *Single Mol.* **2002**, *3*, 275−280.
(11) Shaiu, W.-L.; Vesenka, J.; Jondle, D.; Henderson, E.; Larson, D. D. *Nucleic Acids Res.* **1992**, *11*, 99−103.
(12) Reichert, J.; Csáki, A.; Köhler, J. M.; Fritzsche, W. *Anal. Chem.* **2000**, *72*, 6025−6029.
(13) Hamad-Schifferli, K.; Schwartz, J. J.; Santos, A. T.; Zhang, S.; Jacobson, J. M. *Nature* **2002**, *415*, 152−155.
(14) Liehr, T.; Thoma, K.; Kammler, K.; Gehring, C.; Ekici, A.; Bathke, K. D. *Appl. Cytogenet.* **1995**, *21*, 185−188.
(15) Roider, J.; Hillenkamp, F.; Flotte, T.; Birngruber, R. *Proc. Natl. Acad. Sci. U.S.A.* **1993**, *90*, 8643−8647.
(16) Boyer, D.; Tamarat, P.; Maali, A.; Lounis, B.; Orrit, M. *Science* **2002**, *297*, 1160−1163.
(17) Ito, S.; Yoshikawa, H.; Masuhara, H. *Appl. Phys. Lett.* **2002**, *80*, 482−484.
(18) Kurita, H.; Takami, A.; Koda, S. *Appl. Phys. Lett.* **1998**, *72*, 789−791.
(19) Kreibig, U.; Vollmer, M. *Optical Properties of Metal Clusters*; Springer: Berlin, 1995.
(20) Hacker, G. W. Silver-Enhanced Colloidal Gold for Light Microscopy. In *Colloidal Gold: Principles, Methods, and Applications*; Hayat, M. A., Ed.; Academic Press: New York, 1989; Vol. 1, pp 297−321.
(21) Steinbrück, A.; Csaki, A.; Festag, G.; Fritzsche, W. *Plasmonics* **2006**, *1*, 79−85.
(22) Maubach, G.; Born, D.; Csaki, A.; Fritzsche, W. *Small* **2005**, *1*, 619−624.
(23) Alivisatos, A. P.; Johnsson, K. P.; Peng, X.; Wilson, T. E.; Loweth, C. J.; Bruchez, M. P., Jr.; Schultz, P. G. *Nature* **1996**, *382*, 609−611.
(24) Mirkin, C. A.; Letsinger, R. L.; Mucic, R. C.; Storhoff, J. J. *Nature* **1996**, *382*, 607−609.
(25) Csáki, A.; Möller, R.; Straube, W.; Köhler, J. M.; Fritzsche, W. *Nucleic Acids Res.* **2001**, *29*, e81.
(26) Möller, R.; Csáki, A.; Köhler, J. M.; Fritzsche, W. *Nucleic Acids Res.* **2000**, *28*, e91.
(27) Waye, J. S.; Willard, H. F. *Nucleic Acids Res.* **1987**, *15*, 7549−7569.
(28) Bailey, S. M.; Murnane, J. P. *Nucleic Acids Res.* **2006**, *34*, 2408−2417.
(29) Jing, J.; Reed, J.; Huang, J.; Hu, X.; Clarke, V.; Edington, J.; Housman, D.; Anantharaman, T. S.; Huff, E. J.; Mishra, B.; Porter, B.; Shenker, A.; Wolfson, E.; Hiort, C.; Kantor, R.; Aston, C.; Schwartz, D. C. *Proc. Natl. Acad. Sci. U.S.A.* **1998**, *95*, 8046−8051.
(30) Yokota, H.; Johnson, F.; Lu, H.; Robinson, M.; Belu, A. M.; Garrison, M. D.; Ratner, B. D.; Trask, B. J.; Miller, D. L. *Nucleic Acids Res.* **1997**, *25*, 1064−1070.
(31) Li, J.; Bai, C.; Wang, C.; Zhu, C.; Lin, Z.; Li, Q.; Cao, E. *Nucleic Acids Res.* **1998**, *26*, 4785−4786.
(32) Verma, R. S.; Babu, A. *Human Chromosomes: Manual of Basic Techniques*; Pergamon Press: New York, 1989.
(33) Keren, K.; Soen, Y.; Ben Yoseph, G.; Gilad, R.; Braun, E.; Sivan, U.; Talmon, Y. *Phys. Rev. Lett.* **2002**, *89*, 88103−88111.

NL061966X